iScience

CellPress
OPEN ACCESS

Article

Targeted demand response for mitigating price volatility and enhancing grid reliability in synthetic Texas electricity markets

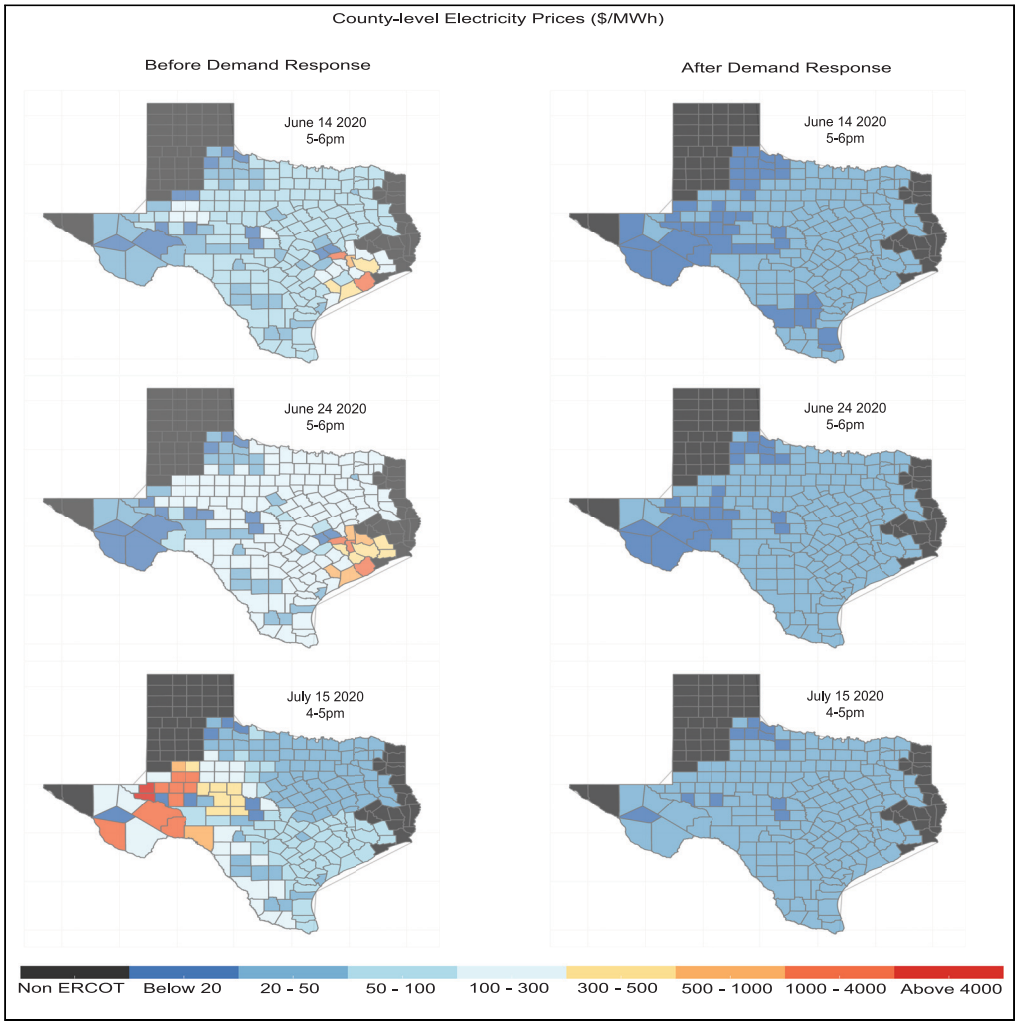

Kiyeob Lee, Xinbo Geng, S. Sivaranjani, Bainan Xia, Hao Ming, Srinivas Shakkottai, Le Xie

le.xie@tamu.edu

Highlights

Demand response holds great potential in enabling reliable renewable-rich electric grids

Large-scale integration of renewable generations causes challenges in system operations

Demand response can mitigate price volatility in renewable-rich electric grids

Targeted demand response, rather than across-the-board DR, is shown to be more effective

Lee et al., iScience 25, 103723
February 18, 2022
https://doi.org/10.1016/j.isci.2021.103723

iScience

CellPress
OPEN ACCESS

Article

Targeted demand response for mitigating price volatility and enhancing grid reliability in synthetic Texas electricity markets

Kiyeob Lee,[1] Xinbo Geng,[1] S. Sivaranjani,[1] Bainan Xia,[2] Hao Ming,[3] Srinivas Shakkottai,[1] and Le Xie[1,4,*]

SUMMARY

Demand response (DR) is rapidly gaining attention as a solution to enhance the grid reliability with deep renewable energy penetration. Although studies have demonstrated the benefits of DR in mitigating price volatility, there is limited work considering the choice of locations for DR for maximal impact. We reveal that very small load reductions at a handful of targeted locations can lead to a significant decrease in price volatility and grid congestion levels based on a synthetic Texas grid model. We achieve this through exploiting the highly nonlinear nature of congestion dynamics and by strategically selecting DR locations. We demonstrate that we can similarly place energy storage to achieve an equivalent impact. Our findings suggest that targeted DR at specific locations, rather than across-the-board DR, can have substantial benefits to the grid. These findings can inform energy policy makers and grid operators how to target DR initiatives for improving grid reliability.

INTRODUCTION

Electricity markets are increasingly facing significant price volatility because of extreme weather events that are becoming more frequent. Furthermore, the large-scale integration of renewable energy poses serious challenges to grid reliability. It has been widely recognized that demand response (DR) holds the potential to integrate consumers in the market at a large scale to smooth out price volatility and mitigate the impact of uncertain renewable energy on grid reliability (Qdr, 2006; Albadi and El-Saadany, 2007, 2008). The purpose of DR is to provide end consumers incentives to change their real-time demand when the system is overly stressed or in an emergency, thereby promoting system-wide operational, economic, and social welfare (Albadi and El-Saadany, 2007). When the demand is very high, there is a risk of not serving the loads, thereby resulting in social welfare losses (Conchado and Linares, 2012). Furthermore, increased carbon emissions may occur during high demand periods for certain generation mixes where more polluting generators such as oil and natural gas are used to meet peak demands (Stoll et al., 2014; Conchado and Linares, 2012). Therefore, DR programs could substantially benefit economic welfare and carbon emissions. Economic assessments suggest that well-designed DR programs may be effective in mitigating these impacts by significantly decreasing price volatility as quantified by locational marginal prices (LMPs) (Walawalkar et al., 2008; Feuerriegel and Neumann, 2014; Asadinejad and Tomsovic, 2017) and carbon emissions (Choi and Thomas, 2012; Van Horn and Apostolopoulou, 2012). From an operational perspective, high demand may result in grid congestion, which may significantly impact grid reliability toward extreme events. Once again, DR programs may hold the potential to enhance grid reliability under such extreme events (Mousavizadeh et al., 2018; Kopsidas and Abogaleela, 2018; Hafiz et al., 2019; Khalili et al., 2020), even if only to blunt their impact to some extent.

However, there are several studies indicating that DR programs, if improperly designed in terms of mechanism or location, can have adverse effects including increased price volatility (Roozbehani et al., 2012) and carbon emissions (Stoll et al., 2014; Nilsson et al., 2017). In particular, owing to the nonlinear dynamics of the power flows and congestion in the grid, demand reduction at certain locations may in fact lead to increased LMPs (Wu, 2013; Yang and Chen, 2009). However, traditional DR studies have typically focused on locations with high LMPs or population centers (Wu, 2013; Zhao and Wu, 2013). In this context, there is limited work actively considering grid dynamics to inform the choice of locations for DR-based load reductions in order to avoid these adverse impacts. Here, we study the impacts of targeted DR to the grid and bridge this gap by developing a machine

[1]Department of Electrical and Computer Engineering, Texas A&M University, College Station, TX 77843, USA

[2]Breakthrough Energy, Kirkland, WA 98033, USA

[3]School of Electrical Engineering, Southeast University, China

[4]Lead contact

*Correspondence: le.xie@tamu.edu

https://doi.org/10.1016/j.isci.2021.103723

learning (ML)-based framework that actively integrates the grid congestion dynamics to carefully select DR locations that can achieve maximum impact on price volatility and grid reliability.

We begin to investigate the DR framework on a large-scale open-source synthetic representation of the Electric Reliability Council of Texas (ERCOT) electricity grid developed in the community (Birchfield et al., 2016; Wu et al., 2021). The synthetic model on the ERCOT grid is one of the largest models (2,000-bus) publicly available to research communities. Moreover, the synthetic model has generator capacities and time series such as hourly demand profiles, wind and solar generation profiles over years taken from the public open-access dataset that statistically match the real ERCOT grid (Xu et al., 2020). Building an electricity market on top of the synthetic grid model, we empirically demonstrate the effectiveness of targeted nodal demand reductions at certain locations due to the nonlinear dynamics of grid congestion. We also demonstrate a counterexample that DR may result in adverse impacts like increased LMPs due to the nonlinear dynamics of grid congestion, motivating the need for carefully targeted DR. We propose a targeted DR framework that employs a ML-based algorithm to select locations where very small targeted load reductions can achieve nonlinear transitions to operating points of the system state that achieve significantly lower price volatility and congestion levels by exploiting the highly nonlinear dynamics of the congestion in the grid. Using this targeted DR framework, we demonstrate that extremely small DR-based load reductions (10.41 MW of a total system load of 48,948 MW) at a carefully targeted handful of locations (10 of 2,000 nodes) can in fact achieve a significant reduction in price volatility, as indicated by an ≈70% decrease, respectively, in mean LMPs (averaged over all locations) over a year, as well as an 80% decrease in grid congestion levels in the ERCOT case study. We further compare the performance of the targeted DR framework with a traditional DR framework, where the DR locations are chosen to be those with maximum LMPs, typically aligned with the major population centers. We demonstrate that targeted DR can achieve a similar reduction in price volatility and grid congestion as compared with traditional DR with only a fraction (≈20%) of the load reduction required by traditional DR. Finally, we show that the ML-based DR algorithm can also be used to determine locations for placement of energy storage to achieve maximum impact on grid reliability, especially in the presence of renewable generation.

Our case study finds that the locations where DR load reductions achieve maximum impact with minimal load reductions could be far from major load or population centers and do not coincide with locations where high LMPs are observed, indicating that the nonlinear dynamics of congestion in the grid play a key role in shaping price volatility and grid reliability. We illustrate this nonlinear dynamics using a simple two-bus example because high dimensions are not possible to draw. These findings can directly inform policy makers in targeting future DR initiatives for maximum impact on operational, economic, and social welfare. In summary, we believe that this is the first work to propose and demonstrate the impact of well-targeted DR schemes that actively exploit the nonlinearities in grid congestion dynamics toward achieving significant reductions in price volatility and grid congestion in electricity markets.

RESULTS

Demand response framework

We begin by developing electricity markets on a synthetic representation of a 2,000-node ERCOT electric grid. Although the synthetic grid model is fictitious since any real grid has privacy and confidentiality requirements, it matches the size, complexity, and characteristics of the actual ERCOT grid (Birchfield et al., 2016) and is one of the largest grid (2,000-node) with publicly available open-access dataset such as time series profiles including hourly demand and renewable profiles. (More details about creation and calibration are given in Method details.) Using day-ahead renewable profiles (forecast estimates), a security-constrained unit commitment (SCUC) problem is solved to determine for day-ahead planning with ballpark estimates that SCUC determines how many and which generating units are committed throughout each day with less precise estimates in advance. This is a standard scheduling problem in power systems as generating units have many physical constraints such as ramping rates to reach a target supply. Then, a security-constrained economic dispatch (SCED) problem is solved in real time with more precise estimates and provides the LMP at every node. In our DR framework, we consider the LMPs obtained every hour from the solution of the SCED problem. The LMP is a basic electricity market price signal ($/MWh) at every location, which can be interpreted as the extra cost incurred to serve an additional unit of load at a particular location. In addition, the dual variables for the transmission capacity constraints in SCED are referred to as shadow prices in the literature, which measure the level of grid congestion and grid reliability. In this work, we are interested in the impacts of targeted DR in terms of LMPs and shadow prices as they represent

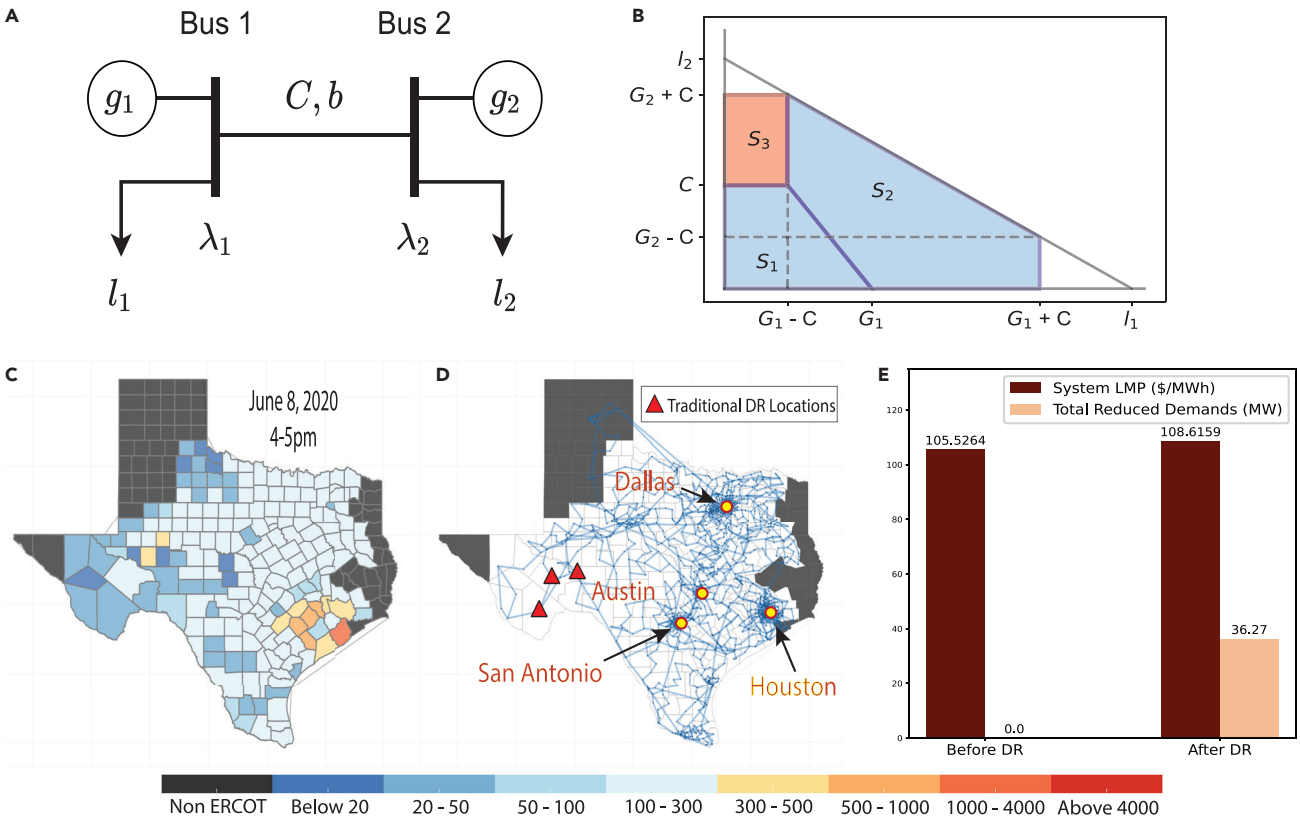

Figure 1. Examples of two-bus networks and a Demand Response event in synthetic Texas electricity markets

(A) Two-bus networks, (B) feasible load sets for two-bus network, (C–E) county-wise locational marginal prices (LMPs) when a DR event happens in the ERCOT market in Texas. Counties are colored by the value of the LMPs, as indicated by the color bar at the bottom. In each county, LMP is averaged over all locations in that county. A counter example of improperly designed DR programs showing adverse effects of increased price volatility.

price volatility and grid reliability. To appeal to a broader audience, a detailed description of the SCUC and SCED problem formulations can be found in Method details. We remark that both SCUC and SCED are repeatedly solved with different timescales. For example, SCUC is typically solved once per day or week with ballpark estimates, and SCED is solved in real time once every 5 min with more precise estimates. After solving SCUC and SCED problems, for this system, we develop a DR framework based on both physical and market constraints (see Method details for the architecture of the DR framework). Physical constraints including fuel-based generating units, renewable generating units, transmission lines, and demand profiles all together determine the operational balance of supply and demand.

We now describe geometric properties of DR that we will exploit in this work. It is commonly known that the feasible nodal load profiles of SCED are a union of polytopes (Jia et al., 2013). Consider a simple two-bus example shown in Figure 1A. The loads are l_1, l_2; the generations are g_1,.g_2; the line capacity is C with line susceptance b; the generation limits are $G1$, $G2$; and LMPs are λ_1, λ_2. When generation costs are linear or quadratic, it can be shown that the feasible load set is the union of three sets S_1, S_2, and S_3 as in Figure 1B where the intersection of interior points is empty. The blue polytopes represent the congestion-free load sets, whereas the red polytope represents congested load sets. Within each polytope, it is known that the LMPs are continuous, whereas it is discontinuous between polytopes. When the nodal demand changes, the solution may move to a different polytope, which is a nonlinear behavior. In our work, we exploit this idea by essentially changing the nodal demand to another demand such that the system state is switched from an undesirable polytope to another desirable polytope. We give a simple example of two-bus networks in which the geometric properties of polytopes look simple because we cannot draw higher dimensional polytopes. However, the geometric properties may be very complicated in a large-scale system as each polytope is characterized by a set of congested lines and a set of marginal generators (Jia et al., 2013).

In general, larger demand reductions are positively correlated with decreased LMPs. However, demand reductions may not always lead to successful DR. Figure 1C illustrates this fact based on a sample DR event from our aforementioned ERCOT test study, where the mean LMP increased from $105/MWh to $108/MWh, although 36 MW of demand was reduced at some selected DR locations. This result demonstrates that demand reductions may lead to adverse effects, such as increased mean LMPs, when DR locations are not carefully selected. Such effects of DR can be attributed to the nonlinear behavior in the system as demonstrated in Figure 1A (two-bus network) that it is possible that the nodal demand profile moves from one polytope to another polytope. Figure 1C provides evidence of this phenomenon, mathematically predicted in earlier work for small systems (Yang and Chen, 2009), through a large-scale real-life test study. In order to prevent such adverse impacts, it is important to design DR programs that explicitly take into account the nonlinear behavior of the system. Along the same vein, it may actually be possible to actively exploit these nonlinear effects to construct well-targeted DR programs that achieve significant LMP reductions with small demand reductions. This is the key idea behind this work. In the following section, we demonstrate how the nonlinearity of the system can be leveraged to design carefully targeted DR that achieves significant reductions in LMPs. We consider the impacts of both traditional DR and ML-based DR proposed in this paper.

At any time period of a day, when the mean LMP (averaged LMP over all locations) or zonal LMP (averaged LMP over all locations in a zone/region) exceeds $100/MWh, then a DR event is called for. There are case studies for DR programs by the New England Independent System Operator (ISO-NE) (Faria et al., 2011) and PJM (Walawalkar et al., 2008), a Regional Transmission Organization (RTO), where these programs used DR threshold points of $100 and $75, respectively. In this work, we chose the threshold as $100, which is also consistent with public data of LMPs released by the ERCOT. Moreover, the typical retail price is $0.10–0.12/kWh (which is equal to $100–120/MWh) in the ERCOT electricity market in 2021. Hence, $100/MWh is around where marginal benefits approximately equal marginal costs for retailers.

When DR events are triggered that the mean LMP is greater than $100/MWh, identify a certain number of locations for DR candidates and reduce the demand at these locations. If the reduced demand profile results in the mean LMP below $100/MWh, the DR event is declared to be successful. Otherwise, a larger demand reduction is carried out at the selected locations or a greater number of locations are selected to participate in DR. This process is repeated until the mean LMP drops below $100/MWh. By iterating this process, there will be a list of successful DR candidate pairs of targeted locations and targeted demand reductions. Such a list is useful because there always is a trade-off between targeted demand reductions and market welfare gains, such as the resulting mean LMP, which can be used by DR program administrators to target appropriate DR measures.

Lastly, the idea of DR is based on the fact that the dual variables (LMPs and shadow prices) are sensitive to the nodal demand changes. Therefore, the system state after DR could become again unstable in principle when there are small perturbations in some locations as noise might push the system back to an undesirable operating state. For example, if nodal demand changes tiny enough to get to a desirable polytope such that it is very close to boundaries between polytopes as shown in Figure 1, then a tiny change could push the system back to the original polytopes. Clearly, it is possible to overcome such issues by requesting more than tiny nodal demand changes. To evaluate sensitivity analysis of DR on the synthetic ERCOT grid model, we added perturbation noise to DR locations incrementally starting from 0 to infinity until the system becomes infeasible. We observed that adding tiny perturbation noise makes the dual variables remain the same, whereas too much perturbation noise makes the system infeasible.

Machine learning-based targeted demand response

We now propose detailed descriptions for ML-based DR framework. As mentioned in the introduction, the impacts of DR can be assessed in the following three contexts: economic, operational, and social welfare gains (Qdr, 2006; Conchado and Linares, 2012; Van Horn and Apostolopoulou, 2012). We focus to quantify the impacts in terms of LMPs and shadow prices in which they characterize price volatility and grid congestion level, respectively.

Besides measuring the impacts of DR to the grid, many studies focused on DR programs on customer ends. To operate DR programs, it is important to know customers' consumption baselines and short-term load and price forecasts. Surveys (Vázquez-Canteli and Nagy, 2019; Antonopoulos et al., 2020) summarize

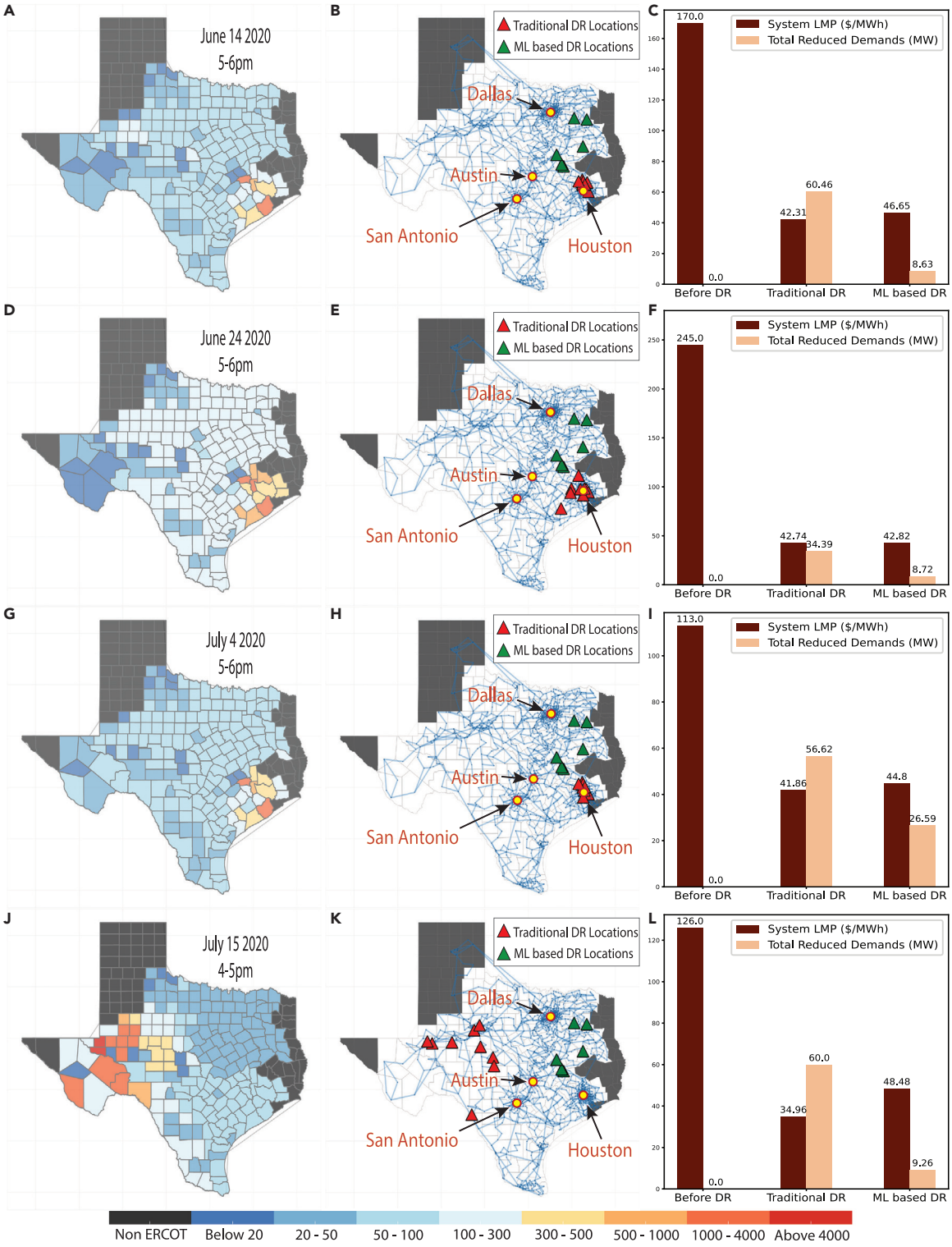

Figure 2. Demand response events in synthetic Texas electricity markets

(A, D, G and J) High LMPs in several counties on each of the 4 days before DR. (B, E, H, and K) Traditional DR and ML-based DR locations to achieve low LMPs (note that traditional DR locations coincide with population centers or high LMPs, whereas ML-based DR locations do not). (C, F, I and L) Significantly decreased LMPs after both traditional DR and ML-based DR for the corresponding time periods and required total reduced demands for successful DR methods.

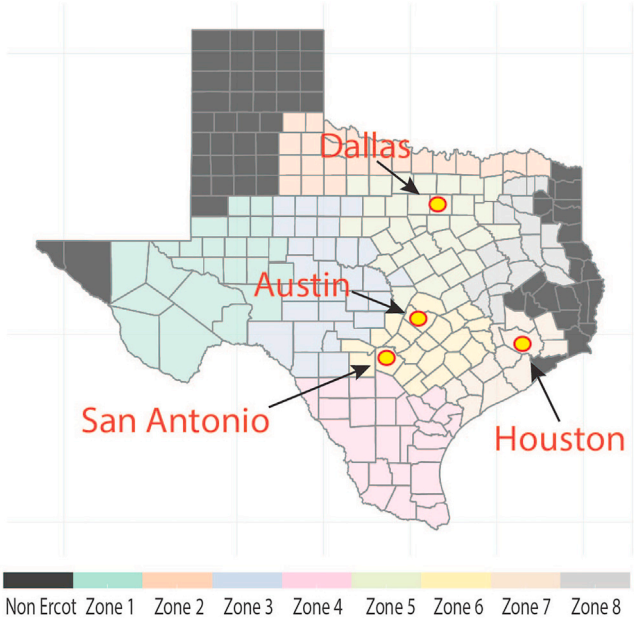

Figure 3. Zonal map of ERCOT electricity markets

The ERCOT grid is visualized on top of the Texas counties map. Counties marked in gray were not part of the ERCOT market during the period considered in this study.

AI/ML algorithms used to predict these variables. On the other hand, this study focuses on the impacts induced by targeted DRs to the grid. Most studies (Wu, 2013; Zhao and Wu, 2013) focused on locations with high LMPs or population centers. This is a natural choice because, otherwise, some participants in electricity ecosystems such as load-serving entities may experience immediate monetary losses when extremely high LMPs are observed. Therefore, there are immediate monetary incentives for some participants to utilize the flexibility of demands from end users at locations with high prices. Moreover, the LMP at each location can be interpreted as an extra cost when an additional unit of demand is added at the location; thus, it is reasonable to reduce demands at locations with high LMPs. Our test study also confirms this wisdom that significant LMP reductions can be obtained by selecting locations with high LMPs (typically situated near large population centers) as DR locations (Figure 2) in a large-scale system on a synthetic ERCOT grid. Furthermore, it is possible to exploit the nonlinearities (Figure 2B) to find alternative locations where DR may have a more significant impact. We develop an ML-based DR framework to achieve these dual objectives.

The simulation time period is over 1 year in 2020 (January 1, 2020 to December 31, 2020), where SCUC is solved once a day and SCED is solved once every hour. Our ML-based DR framework uses one of the simplest ML algorithms called *k*-nearest neighbor (the detailed algorithm is provided in the experimental procedures section). Here, we mainly focus on intuition and the main idea is summarized as follows. Suppose the grid faces a system state x (the nodal demand) that results in high LMPs, we first identify from historical data k-nearest neighborhood of x, denoted by $\tilde{x}$, so that $\tilde{x}$ is close to x and $\tilde{x}$ had low LMPs. DR is essentially moving the system state of the nodal demand x toward $\tilde{x}$ in the hope that the resultant system state has low LMPs. The algorithm identifies a handful of DR locations (a subset of x to move toward $\tilde{x}$), which is 10 of 2,000 in our test study. The intuition to move x toward $\tilde{x}$ is that we know $\tilde{x}$ resulted in low LMPs and are closest to x. Therefore, it may be possible to move a small amount, while achieving a nonlinear jump that results in significantly lower LMPs.

We visualize the impacts of the proposed ML-based DR algorithm using our ERCOT test study in Figure 2. There are 254 counties in Texas, and the power supply in 63 counties was not administered by ERCOT by the time of this study. Each county has multiple locations; hence, the LMP value for each county is averaged over all locations in that county. In Figure 2, the first column represents LMPs before DR during four distinct DR events where the mean LMPs were significantly higher than their typical levels for this system (Figures 2A, 2D, 2G, and 2J). Figure 3 and Table 1 further presents the statistics

Table 1. Several representative DR events to show traditional DR and ML-based DR

		Total reduced demands (MW)	Mean LMP ($/MWh)	Mean shadow price
June 8, 2020 4–5 p.m.	Before DR		105.53	1,170.4
	After traditional DR	30.13	42.00	339.7
	After ML-based DR	8.6	42.08	340.8
June 12, 2020 4–5 p.m.	Before DR		118.11	2,456.7
	After traditional DR	54.96	30.15	157.3
	After ML-based DR	8.49	53.91	813.5
June 14, 2020 5–6 p.m.	Before DR		170.19	3,185.9
	After traditional DR	55.94	42.31	320.0
	After ML-based DR	8.63	46.65	591.8
June 24, 2020 5–6 p.m.	Before DR		245.05	4,868.8
	After traditional DR	55.94	42.73	341.9
	After ML-based DR	8.63	42.82	343.1
July 4, 2020 5–6 p.m.	Before DR		112.79	1,920.1
	After traditional DR	34.39	41.86	324.9
	After ML-based DR	8.72	44.80	519.8
July 8, 2020 4–5 p.m.	Before DR		194.59	4,973.6
	After traditional DR	56.17	49.09	540.0
	After ML-based DR	8.97	55.61	1,011.0
July 15, 2020 4–5 p.m.	Before DR		125.73	4,729.3
	After traditional DR	60.46	34.96	398.8
	After ML-based DR	9.25	48.48	992.6

of the LMP changes, demand reductions, and grid congestion (quantified in terms of shadow prices) for another set of DR events. Finally, Tables 2–4 present the statistics of LMPs, shadow prices, and demand reductions for all DR events through the 1-year period in the case study. For these DR events, we compare the economic and social welfare impacts of traditional DR at locations with high LMPs with that of DR at locations selected by the proposed ML-based algorithm. Both traditional DR and ML-based DR achieve significantly reduced LMPs (75% and 70%, respectively) and shadow prices (91% and 80%, respectively) in these cases. Surprisingly, however, the ML-based DR algorithm achieves welfare gains that are comparable with traditional DR, with only a fraction (<20%) of the total amount of load reductions required to achieve the same impact with traditional DR (Figures 2C, 2F, 2I, 2L and Table 4). Furthermore, we note that the total load reduction required in the ML-based DR algorithm comprises only 10.41 MW out of a total system load of 48,948 MW (Table 4). A closer examination of the DR locations in Figures 2B, 2E, 2H, and 2K reveals another interesting insight—DR locations in the traditional framework that are concentrated in population centers or locations with high LMPs do not remain the same for different DR events, whereas the ML-based DR locations turn out to be the same for each of the different DR events. These two observations confirm the key idea that nonlinearities in the grid play a significant role in the outcomes of DR; the ML-based framework exploits these nonlinearities to select those locations that achieve nonlinear jumps to operating points that result in significant economic and operational welfare gains with very small demand reductions. Interestingly, this study reveals that the locations where DR can achieve maximum impact with minimal demand reductions

Table 2. Statistics of LMP changes of all DR events before/after DR for Zones 1–8

LMP ($/MWh)	Mean	Zone 1	Zone 2	Zone 3	Zone 4	Zone 5	Zone 6	Zone 7	Zone 8
Before DR	165.85	111.08	101.38	103.08	98.83	104.13	128.36	365.62	121.19
After traditional DR	40.08	39.28	35.18	36.07	31.57	36.26	39.67	52.54	37.52
After ML-based DR	50.93	43.36	38.55	39.72	37.08	39.54	44.48	88.11	41.25

Table 3. Statistics of shadow price changes of all DR events, which indicate changes in congestion levels in the grid, before/after DR

Shadow prices	Absolute prices	Standard deviation
Before DR	4,169	7,633.8
After traditional DR	855.7	1,405.6
After ML-based DR	387.9	733.5

may not coincide with the intuitive wisdom of carrying our DR at locations with high LMPs or large population centers. Furthermore, we note that the ML algorithm has another inherent advantage. By construction, the algorithm cannot lead to adverse impacts like increased LMPs, since it actively seeks out operating points with low LMPs.

Machine learning framework for targeted storage placement

Energy storage also holds the potential to benefit operational, market, and social welfare gains because of its flexibility to discharge to the grid when systems are overly stressed and charge back when not. In this sense, energy storage is akin to DR resources. Moreover, energy storage capacity has grown rapidly over the past decade owing to the decrease in battery cell manufacturing costs (Nykvist and Nilsson, 2015). Energy storage also has the potential to mitigate the intermittency and uncertainty induced by limited supply and renewable energy sources. Typically, the most common and traditional approach to mitigating demand peaks and variability of renewable generation is to operate fast-ramping generators such as combined-cycle combustion turbines and gas turbines (Energy, 2010). However, recent works suggest that energy storage with large enough capacity can instead replace fast-ramping traditional generation toward in this context (Su and El Gamal, 2011). Therefore, it is natural to explore if the ML-based DR algorithm proposed in the previous section can also be extended toward choosing locations for energy storage. We explore this question using the same ERCOT case study as in the previous sections. We assume that energy storage resources operate as controllable loads instead of price-responsive loads; that is, batteries can discharge/charge within their capacity limits as needed and do not operate to maximize profits.

Mobility, storage locations, and total capacities together are interrelated. In general, the larger the total capacities, the more the benefit gains that are possible. On the other hand, as shown in Figure 1, it may not always be possible to draw benefit from energy storage if locations are not strategically selected. In this regard, a feature of ML-based DR that was discussed earlier, namely, that it finds a set of locations that remains fixed over almost all DR events, turns out to be a key advantage. Although some energy storage systems are mobile that it is possible to move energy storage to different locations, there are additional burdens in terms of operational time and costs. In this context, ML-based DR locations could be excellent candidate locations for placing energy storage to achieve the same benefit gains as DR programs. Placing storage units at the locations selected by the ML-based DR locations will also provide the advantage of achieving maximum impact on price volatility and grid reliability, while requiring significantly less mobility of energy storage. Moreover, ML-based DR locations will require much less investments in terms of total energy capacity as compared with traditional DR as demonstrated in Figure 3, Tables 2–4; that is, achieving the same level of benefit gains of traditional DR by installing energy storage in traditional DR locations requires nearly five times more total energy capacity, since traditional DR requires nearly five times more demand reductions compared with ML-based DR.

We now demonstrate how the ML-based DR algorithm can be leveraged toward installing energy storage at a few targeted locations to avoid extreme operating points. In our ERCOT test study, we assume that energy storage units are contracted to discharge energy into the grid when DR events are called for and

Table 4. Quantity of DR demand reduction required to achieve the LMP and Shadow Price statistics in Tables 2 and 3

Changes in loads	MW
Total reduced loads in traditional DR	51.49
Total reduced loads in ML-based DR	10.41
Total system loads	48,948

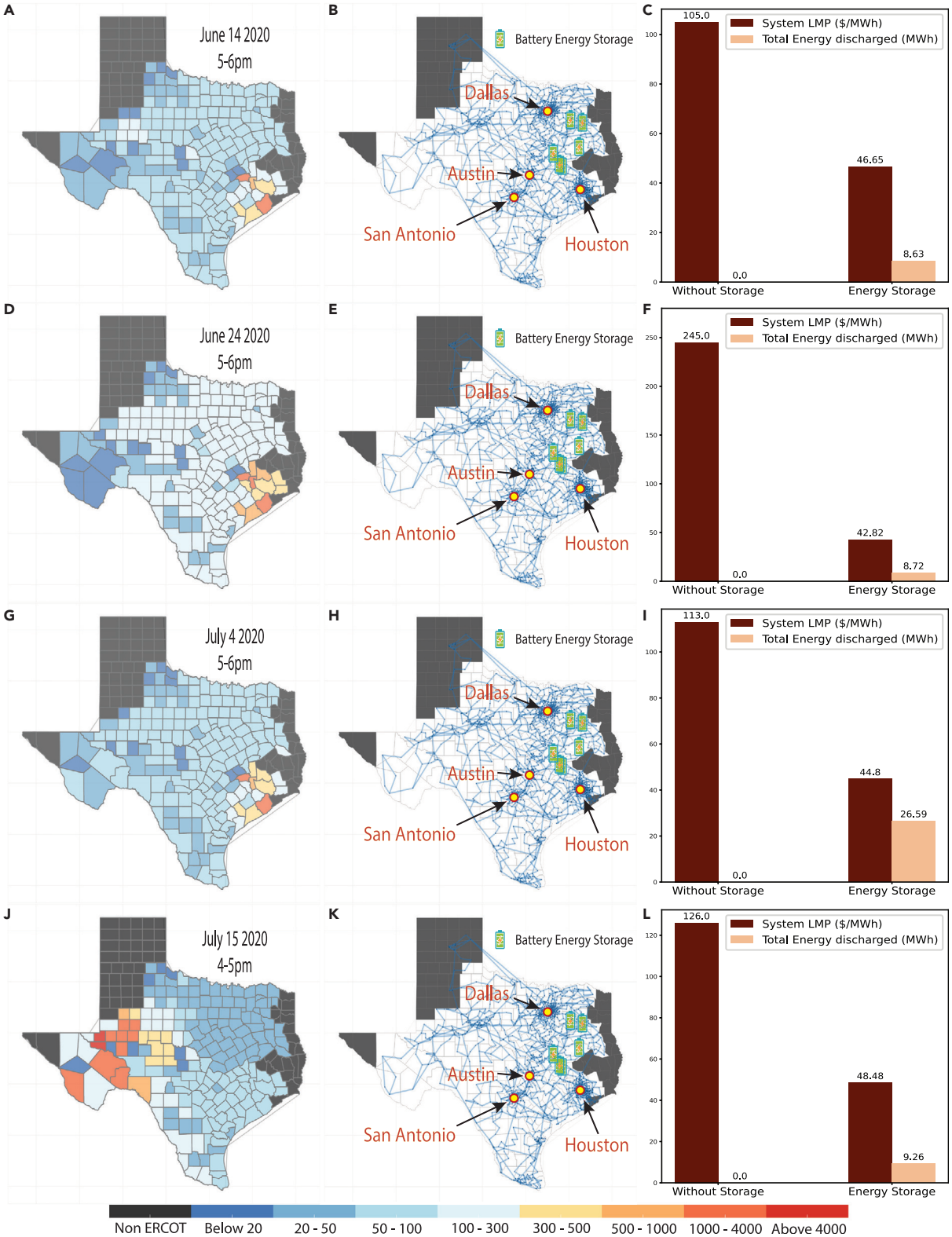

Figure 4. Battery energy storage scenarios in synthetic Texas electricity markets

(A, D, G and J) High LMPs in several counties on each of the 4 days without storage. (B, E, H, and K) Locations of battery energy storage in ML-based DR locations to achieve low LMPs. (C, F, I and L) Significantly decreased LMPs with battery energy storage installed for the corresponding time periods and the total energy discharged.

charge energy back between 12 and 6 AM. In general, energy storage units have multiple parameters such as charging and discharging power rating, energy capacity, charging and discharging efficiency, battery cycle life, battery shelf life, or maintenance costs (Xu et al., 2018). In this work, for simplicity, we assume that the energy storage units all have the following simplified specifications—a charging and discharging power rating of 10 MW, energy capacity of 3 MWh, and charging and discharging efficiency of 95%. Suppose that we install energy storage in the ML-based DR locations as shown in Figure 4. Then, we obtain equivalent welfare gains from energy storage compared with DR programs because installing energy storage in ML-based DR locations can be viewed as equivalent to decreasing demand in the installed locations. Hence, installing energy storage with capacity specified as above in 10 ML-based DR locations is equivalent to participating in ML-based DR program that reduces 8–10 MW in 10 locations. As seen in Figure 4, placing battery energy storage at the ML-based DR locations is equally effective in decreasing mean LMPs that very small amount of energy is discharged from battery energy storage capacity.

DISCUSSION

In this work, we demonstrate both traditional DR and ML-based frameworks in a large-scale system on the synthetic ERCOT grid to understand targeted DR that achieves reductions in price volatility and grid congestion in Texas electricity markets. We also showed how this framework can be used to determine locations for battery energy storage to achieve excellent impacts on grid reliability, as the grid transitions to very large-scale renewable integration. Our findings demonstrate that very small but highly targeted DR, rather than across-the-board DR, can have a significant impact on decreasing price volatility and improving grid reliability in Texas electricity markets. Furthermore, we demonstrate that considering the nonlinear grid dynamics can also be actively exploited toward choosing targeted locations for DR and can achieve excellent impacts, as compared with the typical wisdom of targeting DR schemes toward large population centers or locations with high price volatility. These findings can inform energy policy makers and grid operators on how to target DR initiatives for price volatility as well as the operational reliability. The recent Federal Energy Regulatory Commission (FERC) order 2222 in the United States has paved the way for distributed energy resources, including DR providers and storage resources, to participate in the capacity, energy, and ancillary services markets. In this context, this work will directly inform policy makers on how DR participation mechanisms can be targeted in these emerging market structures.

Limitations of the study

The essential idea of DR is based on the fact that the dual variables (LMPs and shadow prices) are sensitive to the nodal demand changes. Therefore, the system state after DR could become again unstable in principle when there are small perturbations in some locations as noise might push the system back to an undesirable operating state. On the other hand, DR is expected to gain more attention owing to increasing adoption of renewable generations and electric vehicle fleets as they both pose challenges and opportunities to the future grid.

STAR★METHODS

Detailed methods are provided in the online version of this paper and include the following:

- KEY RESOURCES TABLE
- RESOURCE AVAILABILITY
  - Lead contact
  - Materials availability
  - Data and code availability
- METHOD DETAILS
  - Synthetic grid-creation and calibration
  - Architecture of DR frameworks
  - Sensitivity analysis of the mean LMP on all DR events
  - Demand response algorithm
  - Security-constrained unit commitment (SCUC) and security-constrained economic dispatch (SCED)
  - Security-constrained economic dispatch (SCED)
  - Security-constrained unit commitment (SCUC)

ACKNOWLEDGMENTS

The work of X.G., K.L., S. Sivaranjani, S. Shakkottai, and L.X. is supported in part by NSF, United States, CCF-1934904, ECCS-2038963, ECCS-2035688, CPS-2038963, OAC-1934675, and Breakthrough Energy Sciences. The work of H.M. was conducted during his PhD at Texas A&M University.

AUTHOR CONTRIBUTIONS

Conceptualization, L.X. and S. Shakkottai; methodology, X.G. and K.L.; investigation, K.L., X.G., S. Sivaranjani, B.X., H.M., S. Shakkottai, and L.X.; writing – original draft, K.L., X.G., S. Sivaranjani, B.X., H.M., S. Shakkottai, and L.X.; writing – review & editing, K.L., S. Sivaranjani, and L.X.; funding acquisition, L.X. and S. Shakkottai; resources, L.X. and S. Shakkottai; supervision, L.X. and S. Shakkottai.

DECLARATION OF INTERESTS

The authors declare no competing interests.

Received: May 17, 2021
Revised: November 18, 2021
Accepted: December 27, 2021
Published: February 18, 2022

REFERENCES

Administration, U.E.I. (2019). Form EIA-923. https://www.eia.gov/electricity/data/eia923/.

Albadi, M.H., and El-Saadany, E.F. (2007). Demand response in electricity markets: an overview. In 2007 IEEE Power Engineering Society General Meeting (IEEE), pp. 1–5.

Albadi, M.H., and El-Saadany, E.F. (2008). A summary of demand response in electricity markets. Electric Power Syst. Res. *78*, 1989–1996.

Antonopoulos, I., Robu, V., Couraud, B., Kirli, D., Norbu, S., Kiprakis, A., Flynn, D., Elizondo-Gonzalez, S., and Wattam, S. (2020). Artificial intelligence and machine learning approaches to energy demand-side response: a systematic review. Renew. Sustain. Energy Rev. *130*, 109899.

Asadinejad, A., and Tomsovic, K. (2017). Optimal use of incentive and price based demand response to reduce costs and price volatility. Electric Power Syst. Res. *144*, 215–223.

Birchfield, A.B., Xu, T., Gegner, K.M., Shetye, K.S., and Overbye, T.J. (2016). Grid structural characteristics as validation criteria for synthetic networks. IEEE Trans. Power Syst. *32*, 3258–3265.

Choi, D.G., and Thomas, V.M. (2012). An electricity generation planning model incorporating demand response. Energy Policy *42*, 429–441.

Conchado, A., and Linares, P. (2012). The economic impact of demand-response programs on power systems. a survey of the state of the art. In Handbook of Networks in Power Systems I (Springer), pp. 281–301.

Electric Reliability Council of Texas (2021). Load. http://www.ercot.com/gridinfo/load.

Energy, G. (2010). Western Wind and Solar Integration Study, Technical Report (National Renewable Energy Lab.(NREL)).

Faria, P., Morais, H., Vale, Z., and Ferreira, J. (2011). Lmp triggered real time demand response events. In 2011 8th International Conference on the European Energy Market (EEM) (IEEE), pp. 45–50.

Feuerriegel, S., and Neumann, D. (2014). Measuring the financial impact of demand response for electricity retailers. Energy Policy *65*, 359–368.

Gurobi Optimization, LLC (2021). Gurobi Optimizer Reference Manual. https://www.gurobi.com.

Hafiz, F., Chen, B., Chen, C., de Queiroz, A.R., and Husain, I. (2019). Utilising demand response for distribution service restoration to achieve grid resiliency against natural disasters. IET Generation, Transm. Distribution *13*, 2942–2950.

Jia, L., Kim, J., Thomas, R.J., and Tong, L. (2013). Impact of data quality on real-time locational marginal price. IEEE Trans. Power Syst. *29*, 627–636.

Khalili, T., Bidram, A., and Reno, M.J. (2020). Impact study of demand response program on the resilience of dynamic clustered distribution systems. IET Generation, Transm. Distribution *14*, 5230–5238.

Kopsidas, K., and Abogaleela, M. (2018). Utilizing demand response to improve network reliability and ageing resilience. IEEE Trans. Power Systems *34*, 2216–2227.

Lee, K., Geng, X., Sivaranjani, S., Xia, B., Ming, H., Shakkottai, S., and Xie, L. (2021). Github repository for demand response framework of synthetic ERCOT network. https://github.com/tamu-engineering-research/demandresponse.

Mousavizadeh, S., Haghifam, M.-R., and Shariatkhah, M.-H. (2018). A linear two-stage method for resiliency analysis in distribution systems considering renewable energy and demand response resources. Appl. Energ. *211*, 443–460.

Nilsson, A., Stoll, P., and Brandt, N. (2017). Assessing the impact of real-time price visualization on residential electricity consumption, costs, and carbon emissions. Resour. Conservat. Recycling *124*, 152–161.

Nykvist, B., and Nilsson, M. (2015). Rapidly falling costs of battery packs for electric vehicles. Nat. Clim. Change *5*, 329–332.

Qdr, Q. (2006). Benefits of Demand Response in Electricity Markets and Recommendations for Achieving Them (US Dept. Energy).

Roozbehani, M., Dahleh, M.A., and Mitter, S.K. (2012). Volatility of power grids under real-time pricing. IEEE Trans. Power Syst. *27*, 1926–1940.

Stoll, P., Brandt, N., and Nordström, L. (2014). Including dynamic co2 intensity with demand response. Energy Policy *65*, 490–500.

Su, H.-I., and El Gamal, A. (2011). Modeling and analysis of the role of fast-response energy storage in the smart grid. In 2011 49th Annual Allerton Conference on Communication, Control, and Computing (Allerton) (IEEE), pp. 719–726.

The Electric Reliability Council of Texas (2021). Maps. http://www.ercot.com/news/mediakit/maps.

Van Horn, K.E., and Apostolopoulou, D. (2012). Assessing demand response resource locational impacts on system-wide carbon emissions reductions. In 2012 North American Power Symposium (NAPS) (IEEE), pp. 1–6.

Vázquez-Canteli, J.R., and Nagy, Z. (2019). Reinforcement learning for demand response: a review of algorithms and modeling techniques. Appl. Energ. *235*, 1072–1089.

Walawalkar, R., Blumsack, S., Apt, J., and Fernands, S. (2008). An economic welfare analysis of demand response in the PJM electricity market. Energy Policy *36*, 3692–3702.

Wu, D., Zheng, X., Xu, Y., Olsen, D., Xia, B., Singh, C., and Xie, L. (2021). An open-source extendable model and corrective measure assessment of the 2021 Texas power outage. Adv. Appl. Energy *4*, 100056.

Wu, L. (2013). Impact of price-based demand response on market clearing and locational marginal prices. IET Generation, Transm. Distribut. *7*, 1087–1095.

Xu, B., Shi, Y., Kirschen, D.S., and Zhang, B. (2018). Optimal battery participation in frequency regulation markets. IEEE Trans. Power Syst. *33*, 6715–6725.

Xu, Y., Myhrvold, N., Sivam, D., Mueller, K., Olsen, D.J., Xia, B., Livengood, D., Hunt, V., d'Orfeuil, B.R., Muldrew, D., et al. (2020). Us test system with high spatial and temporal resolution for renewable integration studies. In 2020 IEEE Power & Energy Society General Meeting (PESGM) (IEEE), pp. 1–5.

Yang, D., and Chen, Y. (2009). Demand response and market performance in power economics. In 2009 IEEE Power & Energy Society General Meeting (IEEE), pp. 1–6.

Zhao, Z., and Wu, L. (2013). Impacts of high penetration wind generation and demand response on LMPs in day-ahead market. IEEE Trans. Smart Grid *5*, 220–229.

Zimmerman, R.D., Murillo-Sánchez, C.E., and Thomas, R.J. (2010). Matpower: steady-state operations, planning, and analysis tools for power systems research and education. IEEE Trans. Power Syst. *26*, 12–19.

STAR★METHODS

KEY RESOURCES TABLE

REAGENT or RESOURCE	SOURCE	IDENTIFIER
Deposited data		
Synthetic Texas Grid	(Birchfield et al., 2016)	http://electricgrids.engr.tamu.edu/
Time series profiles	(Xu et al., 2020)	https://zenodo.org/record/4538590
Software and algorithms		
MatPower	(Zimmerman et al., 2010)	https://matpower.org/
Gurobi	(Gurobi Optimization, LLC, 2021)	https://www.gurobi.com/
Demand Response Framework	This paper	(GitHub: Lee et al., 2021)

RESOURCE AVAILABILITY

Lead contact

Further information and requests for resources and materials should be directed to and will be fulfilled by the Lead Contact, Dr. Le Xie (le.xie@tamu.edu).

Materials availability

No materials were used in this study.

Data and code availability

- This paper only analyzes publicly available data. Sources of dataset are listed in the key resources table.
- Demand Response Framework is built on MatPower (Zimmerman et al., 2010) which is a Matlab package for solving power system simulations. While it is not necessary, the framework takes advantage of Gurobi (Gurobi Optimization, LLC, 2021), which provides free academic licenses, for faster computation of power flow simulations. All code for Demand Response Framework is publicly available on Github (Lee et al., 2021).
- Any additional information required to reanalyze the data reported in this paper is available from the lead contact upon request.

METHOD DETAILS

Synthetic grid-creation and calibration

A U.S. test system with high spatial and temporal resolution is utilized for the DR case study (Xu et al., 2020). This existing open-access test system is built using only publicly available data sets. The high granularity of the model aligns with the need of having accurate statistics of the power grid infrastructure and capturing the time series dynamics of demand and variable resources in the present work. The synthetic grid model in this study is adapted from the ERCOT part of the U.S. test system with fine-tuned parameters. Note that multiple versions of the test system are available (Xu et al., 2020), which are built on different years of raw data. The year 2020 is selected here to make the study best represent current reality. To provide a better understanding of how the synthetic baseline network is constructed, how the input profiles are generated, and how the model is calibrated, a brief recap of the existing content (Xu et al., 2020) together with detailed descriptions of the specific modifications on the model in this study are provided in the rest of this section.

System topology. The system topology is adopted from the synthetic Texas 2,000-bus grid as described in the literature (Birchfield et al., 2016). The original motivation of the synthetic grid model is to provide a transparent system without any confidential information that statistically matches the real grid. Thus, this test system is well-suited to our DR case study.

Generator capacity. The original capacities of the generator inventory in the model are designed based on the public information pertaining to the year 2016 (Birchfield et al., 2016). Major new generator units and retirements up to 2019 are captured with the whole generator fleet scaled up to match the total capacity at the beginning of 2020 by type and ERCOT weather zone (The Electric Reliability Council of Texas, 2021) in the 2020 test system (Xu et al., 2020).

Generator cost curve. Quadratic cost curves for fossil fuel generators such as natural gas and coal are provided in the original model (Birchfield et al., 2016). Cost curves of different types of generators in each state are scaled by constant factors to make the capacity-weighted average of electricity prices agree with historical data (Xu et al., 2020). During the simulations in the present study, the quadratic cost curves are transformed into 10-piece (or more) piece-wise linear cost curves to improve the computational performance of solving Security-Constrained Unit Commitment (SCUC) and maintain realistic cost estimations of generation.

Time series profiles. Hourly zonal demand, per-plant solar, wind, and hydro profiles which are compatible with the test system (Xu et al., 2020) are provided in the open-access data set. Demand profiles are generated based on historical time series profiles from ERCOT (Electric Reliability Council of Texas, 2021). Geographic load distribution in the synthetic network is provided based on the demographic information of ZIP codes (Birchfield et al., 2016). Renewable profiles are generated based on historical weather traces such as wind speed and solar irradiance from public available data sets, whereas hydro profiles are composed by historical hourly data of real hydroelectric dams and monthly net generation from EIA Form 923 (Administration, 2019). Detailed methodologies and data sources are described in the literature (Xu et al., 2020).

Calibration. The U.S. test system is calibrated by comparing the historical and simulated results of the state-level generation mix obtained by running a full-year production cost model (Xu et al., 2020). In particular, for this study, the statistics of historical and simulated results of Locational Marginal Prices (LMP) are compared for model calibration.

Feasibility check. The existing test system is tuned to be year-long feasible by running a multi-period DC Optimal Power Flow (OPF) in different scenarios (Xu et al., 2020). However, SCUC induces more restrictive conditions in the optimization. The total demand is further scaled down by 4% on days 221–224 in order to achieve feasibility, which we believe is innocuous to the main conclusions of the present work.

Architecture of DR frameworks

Figure shows the architecture of the basic DR framework. Grid operations are based on generator unit schedules, renewable generator profiles, demand profiles, and DR contracts included to describe the DR programs in the market. When the mean LMP is not expected to be higher than $100, the electricity market simply cleared; otherwise, DR program administrators contact DR contractors to perform demand shaping in order to regulate the mean LMP to less than $100. If the optimal scheduling with demand shaping is successful, then the market is cleared with demand reductions.

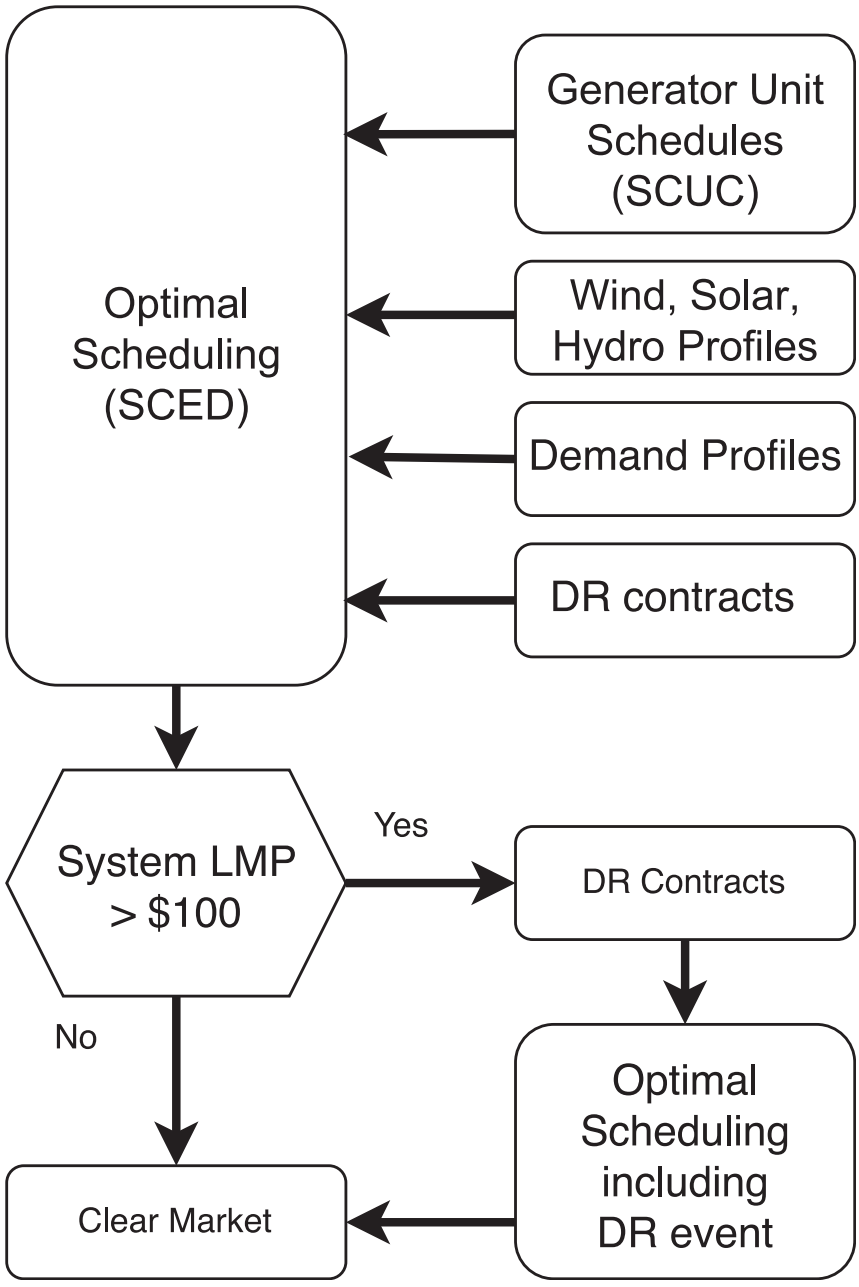

Architecture of the basic DR framework

Optimal scheduling (SCED) is solved in real time (or every 5 min), whereas generator unit schedules (SCUC) are solved 1 day ahead. Details on SCUC and SCED are given in method details.

Sensitivity analysis of the mean LMP on all DR events

Recall from Figure 3 that ML-based DR requires 10.41MW nodal demand changes in average for all DR events. That is, given a nodal demand x with high mean LMP before DR, the mean LMP becomes low when 10.41MW is removed from x. We added both positive and negative perturbation noise to the nodal demand x. This is summarized in Figure where it shows the sensitivity of LMP with respect to noise as the perturbation noise increases from x-10 MW to infinity. Again, we note that the essential idea of demand response is based on the fact that the dual variables (LMPs and shadow prices) are sensitivity to the nodal demand changes.

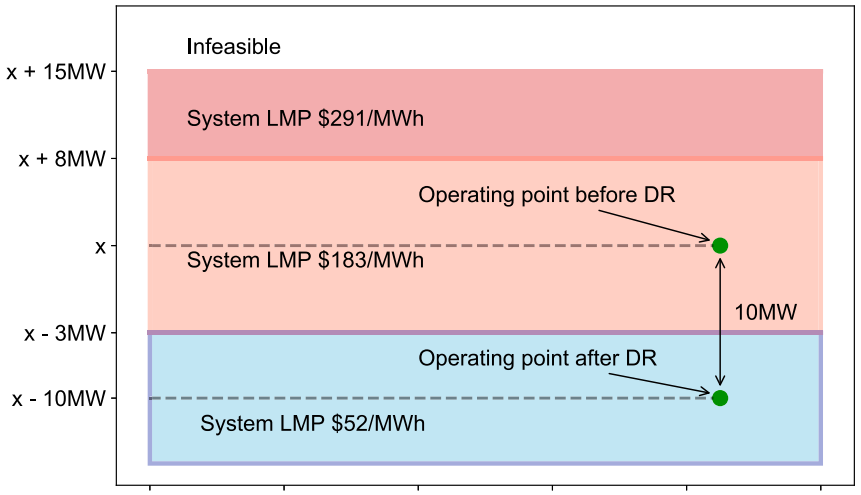

Sensitivity of the mean LMP on DR events

Demand response algorithm

We now describe the ML-based DR framework implemented using the pseudo-code provided in Algorithms 1 and 2. In order to frame proper DR programs, we first start with the simulation setup in our case study. An open-source synthetic representation of the ERCOT electricity grid is built by communities only using publicly available data sets. The high granularity of the model (Birchfield et al., 2016; Wu et al., 2021) aligns with the need of having accurate statistics of the power grid infrastructure and capturing the time series dynamics of demand and variable resources in the present work. As described above in MEthod Details, the synthetic grid model in this study is adapted from the ERCOT part of the U.S. test system with fine-tuned parameters. To provide electric services in the ERCOT electricity grid, a security-constrained unit commitment (SCUC) problem is solved one day ahead and a security-constrained economic dispatch (SCED) is solved in real-time (More details on SCUC and SCED are provided below). Thus, we solve SCUC and SCED for each day at appropriate time, and open DR programs if the resulting mean LMP is higher than $100 for any time of the day.

We define a demand profile as a set of positive demands over locations and assume that there is a collection of demand profiles accumulated over time. We divide the collection of demand profiles into two distinct sets, namely a good set S_g and a bad set S_b. Each demand profile is classified into a good set S_g if the demand profile results in low mean LMP (mean LMP is less than $100) and is classified into a bad set S_b if the demand profile results in high mean LMP (mean LMP is higher than $100). Any new demand profile is also classified based on this rule.

When a new demand profile denoted by new_d is observed to belong to S_b, the traditional DR framework focus exclusively on lowering demands in new_d at locations with population centers or high LMPs. Unlike traditional DR, our ML-based DR algorithm utilizes S_g; given a new demand profile new_d that belongs to S_b, we compute its distance from all elements of S_g - these distances indicate how far new_d is from all good demand profiles. Since S_g is a set of demand profiles with mean LMPs less than $100, the ML-based DR algorithm reduce demands in a few locations in new_d toward so that new_d can be classified into S_g, i.e., results in mean LMPs less than $100. Note that we can only reduce demands in a small number of locations. Therefore, we consider ten locations that have the largest distance from S_g. Also, the number of elements in S_g could be very large; therefore, we choose to consider k-nearest-neighbors in S_g, where k = 20.

Security-constrained unit commitment (SCUC) and security-constrained economic dispatch (SCED)

Nomenclature. Here, we establish some notations and describe the SCUC and problems. The sets of locations (buses), transmission lines, generators, wind farms, and loads are denoted by N, ε, g, W, L respectively.

Algorithm 1. SCUC and SCED

for each day **do**

Solve SCUC with renewable unit profiles and demand profiles

for each hour h = 1:24 **do**

Solve SCED with unit schedules, profiles and demand profiles

Let demand profiles be denoted as demand(B) which is a vector of size 2000 locations

if Mean LMP at hour h $\geq$ \$100 **then**

Perform Algorithm 2 with input : original_demand(B) := demand(B)

end if

end for

end for

Decision *variables in both SCUC and SCED*:

- g_i [t]: MW output of generator *i* at time *t*;
- p_i [t]: net MW power injection at bus *i* at time *t*;
- θ_i [t]: voltage angle of bus *i* at time *t*;
- f_{ij} [t]: power flow on line (i, j) at time *t*.

Decision variables in SCUC:

Algorithm 2. Demand Response

Parameters : k = 20

Input : original_demand(B)

Compute L1 distance between original_demand(B) and all other load profiles in the library

Identify 20 nearest_neighbors to original_demand(B) by sorting out L1 distance vector in ascending order (closest to farthest)

for each nearest_neighbor = 1:k **do**

Find 10 buses denoted as DR_BUS that have the most differences in demands between original_demand(B) and nearest_neighbor

for i = 0.85 : 0.01 : 0.99 **do**

reduced_original_demand(B) = original_demand(B)

reduced_original_demand(DR_BUS) = original_demand(DR_BUS) * i

Solve SCED with reduced_original_demand(B)

end for

if Mean LMP < \$100 **then**

DR is successful. STOP

end if

end for

- $z_i[t] \in \{0,1\}$: commitment (on/off states) decisions; $z_i[t] = 1$ if generator i is on at time t;
- $u_i[t] \in \{0,1\}$: generator i is turned on at time t if $u_i[t] = 1$;
- $v_i[t] \in \{0,1\}$: generator i is turned off at time t if $v_i[t] = 1$.

Parameters and constants:

- $c_i^g(\bullet)$: (piecewise linear or quadratic) cost function of generator i;
- c_i^z: no load cost of generator i;
- c_i^u: startup cost coefficient of generator i;
- c_i^v: shutdown cost coefficient of generator i;
- $d_i[t]$: forecast of load at bus i at time t;
- $\overline{g}_i, \underline{g}_i$: MW upper/lower bounds of generator i;
- $g_i[0]$: generation level of generator i at the beginning of operation planning horizon ($t = 0$);
- $\overline{\theta}_i, \underline{\theta}_i$: upper/lower bounds on voltage angles at bus i;
- $\overline{r}_i, \underline{r}_i$: ramping upper/lower bounds of generator i;
- $\overline{f}_{ij}, \underline{f}_{ij}$: upper/lower bounds on flow of line (i,j);
- $\underline{u}_i, \underline{v}_i$: minimum on (off) time for generator i
- x_{ij}: reactance of line (i,j).

Security-constrained economic dispatch (SCED)

$$\text{minimize} \quad \sum_{t=1}^{n_t} \sum_{i \in \mathcal{G}} c_i^g(g_i[t]) \tag{Equation 1a}$$

$$\text{subject to} \quad p_i[t] = g_i[t] - d_i[t] : \quad (\lambda_i[t]) \quad i \in \mathcal{N};\ t = 1,2,\cdots,n_t. \tag{Equation 1b}$$

$$f_{ij}[t] = \frac{\theta_i[t] - \theta_j[t]}{x_{ij}} \quad (i,j) \in \mathcal{E};\ t = 1,2,\cdots,n_t. \tag{Equation 1c}$$

$$p_i[t] = \sum_{(i,j) \in \mathcal{E}} f_{ij}[t] \quad i \in \mathcal{N};\ (i,j) \in \mathcal{E};\ t = 1,2,\cdots,n_t. \tag{Equation 1d}$$

$$\underline{f}_{ij} \le f_{ij}[t] \le \overline{f}_{ij} \quad : (\mu_{ij}[t]) \quad (i,j) \in \mathcal{E};\ t = 1,2,\cdots,n_t. \tag{Equation 1e}$$

$$\underline{\theta}_i \le \theta_i[t] \le \overline{\theta}_i \quad i \in \mathcal{N};\ t = 1,2,\cdots,n_t. \tag{Equation 1f}$$

$$\underline{r}_i \le g_i[t] - g_i[t-1] \le \overline{r}_i \quad i \in \mathcal{G};\ t = 1,2,\cdots,n_t. \tag{Equation 1g}$$

$$\underline{g}_i \le g_i[t] \le \overline{g}_i \quad i \in \mathcal{G};\ t = 1,2,\cdots,n_t. \tag{Equation 1h}$$

Security-Constrained Economic Dispatch (SCED) seeks the optimal generation that minimizes total costs in the upcoming *nt* snapshots. The main decision variables are the MW outputs of generators $g_i[t]$. Given values of $g_i[t]$, the voltage angles $\theta_i[t]$, nodal MW injections $p_i[t] p_i[t]$, and line flows $f_{jj}[t]$ are determined by equality constraints (Equations 1b), (1c) and (1d). Security constraints ensure: transmission line flow within limits (Equation 1e), voltage angles within limits (Equation 1f), generation capacity limits (Equation 1h), and ramping limits (Equation 1g).

The SCED formulation (1) also provides some critical dual variables. The dual variables for the transmission capacity constraints, which are often referred to as *transmission shadow prices* in the literature, are denoted by $\mu_{ij}[t]$ in (Equation 1e). The dual variables $\lambda_i[t]$ for the nodal balancing constraint (Equation 1b) are called *locational marginal prices* (LMPs) in electricity markets. As their name suggests, LMPs $\lambda_i[t]$ represent the marginal value of one additional unit of demand $d_i[t]$ at bus i at time t. Since SCED is often the key component of *real-time* electricity market, we term the LMPs $\lambda_i[t]$ of SCED as *real-time prices*. Also note that for a multi-period look-ahead SCED formulation (1), only the dual variables for the first snapshot $t = 1$ (i.e., $\lambda_i[t]$) are used for pricing and settlement purposes, and the prices $\lambda_i[t]$ ($t = 2,3,\ ,n_t$) are only advisory.

Security-constrained unit commitment (SCUC)

$$\text{minimize} \quad \sum_{t=1}^{T}\sum_{i\in\mathcal{G}} c_i^g(g_i[t]) + c_i^z z[t] + c_i^u u[t] + c_i^v v[t] \tag{Equation 2a}$$

$$\text{subject to} \quad p_i[t] = g_i[t] - d_i[t] \quad : (\lambda_i[t]) \quad i\in\mathcal{N};\ t=1,2,\cdots,T. \tag{Equation 2b}$$

$$p_i[t] = \sum_{(i,j)\in\mathcal{E}} f_{ij}[t] \quad i\in\mathcal{N};\ (i,j)\in\mathcal{E};\ t=1,2,\cdots,T. \tag{Equation 2c}$$

$$\underline{f}_{ij} \le f_{ij}[t] \le \overline{f}_{ij} \quad : (\mu_{ij}[t]) \quad (i,j)\in\mathcal{E};\ t=1,2,\cdots,T. \tag{Equation 2d}$$

$$f_{ij}[t] = \frac{\theta_i[t] - \theta_j[t]}{x_{ij}} \quad (i,j)\in\mathcal{E};\ t=1,2,\cdots,T. \tag{Equation 2e}$$

$$\underline{r}_i \le g_i[t] - g_i[t-1] \le \overline{r}_i \quad i\in\mathcal{G};\ t=1,2,\cdots,T. \tag{Equation 2f}$$

$$z_i[t]\cdot\underline{g}_i \le g_i[t] \le z_i[t]\cdot\overline{g}_i \quad i\in\mathcal{G};\ t=1,2,\cdots,T. \tag{Equation 2g}$$

$$u_i[t] \ge z_i[t] - z_i[t-1] \quad i\in\mathcal{G};\ t=1,2,\cdots,T. \tag{Equation 2h}$$

$$v_i[t] \ge z_i[t-1] - z_i[t] \quad i\in\mathcal{G};\ t=1,2,\cdots,T. \tag{Equation 2i}$$

$$z_i[t] - z_i[t-1] \le z_i[\iota], \quad \iota\in\left[t+1, \min\left\{t+\underline{u}_i - 1, T\right\}\right],\ t=2,3,\cdots,T. \tag{Equation 2j}$$

$$z_i[t-1] - z_i[t] \le 1 - z_i[\iota], \quad \iota\in\left[t+1, \min\left\{t+\underline{v}_i - 1, T\right\}\right],\ t=2,3,\cdots,T. \tag{Equation 2k}$$

The objective of SCUC (2) is to find the optimal commitment $z_i[t]$ and dispatch decisions $g_i[t]$ that minimize the total cost, which includes no-load costs $c_i^z z_i[t]$, startup costs $c_i^u u_i[t]$, shutdown costs $c_i^v v_i[t]$, and generation costs $c_i^g(g_i[t])$. Note that constraints (Equations 2b, 2c, 2d, 2e, 2f, and 2g) in SCUC are the same as the constraints (Equations 1b, 1c, 1d, 1e, 1f, and 1g) in SCED. Constraint (Equation 2g) differs from (Equation 1h) by adding the commitment variable $z_i[t]$. When generator i is not committed, i.e., $z_i[t] = 0$, (Equation 2g) forces $g_i[t] = 0$. When generator i is committed, i.e., $z_i[t] = 1$, (Equation 2g) is the same as (Equation 1h). Constraints (Equations 2h and 2i) are the logistic constraints pertaining to commitment $z_i[t]$, and startup and shutdown decisions ($u_i[t]$, $v_i[t]$). When generator i is turned on at time t, i.e., $z_i[t\text{-}1] = 0$ but $z_i[t\text{-}1] = 1$; then, constraint (Equation 2h) forces $u_i[t] = 1$. When generator i is turned off at time t, i.e., $z_i[t\text{-}1] = 1$ but $z_i[t] = 0$, constraint (Equation 2h) forces $v_i[t] = 1$. Minimum on/off time constraints for all generators are in (Equations 2j and 2k). Similar to SCED, we also provide critical dual variables of SCUC in (Equation 2b). Since SCUC lies at the heart of *day-ahead* electricity market, we term LMPs $\lambda_i[t]$ of SCUC as *day-ahead prices*.

Although the SCUC and SCED formulations share similar constraints, we would like to point out two major differences. First, SCED is solved in real-time (or 5 minutes before), while SCUC is often solved one day ahead. Consequently, SCUC incorporates the *day-ahead* wind and load forecast, while SCED takes updated and more accurate *real-time* predictions of load and wind generation into account. Second, only the LMPs of the first snapshot $\lambda_i[1]$ in SCED are used for pricing and settlement purposes, while all *day-ahead prices* ($\lambda_i[t]$ s in (Equation 2b)) will be used for settlement.